# PARALLEL INTERLEAVED CONVERTERS AND DYNAMIC RESISTOR IN A DFIG WIND TURBINE DURING THREE PHASE FAULT

**[1]P. Thulasi , [2]S. Abbas Ali**
[1]PG Student, Department of Electrical & Electronics Engineering, JNTU College of Engineering, Ananthapuramu, A.P., India
[2]Lecturer, Department of Electrical & Electronics Engineering, JNTU College of Engineering, Ananthapuramu, A.P., India

***Abstract:*** ***The fast development of wind power generation brings new requirements for wind turbine integration into the network. After clearance of an external short circuit fault, grid-connected wind turbines should restore their normal operation without power loss caused by disconnections. During the fault by flowing the high current for a several micro seconds transient operations are very crucial for high power insulated-gate bipolar transistor modules. Therefore, the ability for doubly fed induction generator (DFIG) variable speed wind turbine power converters to withstand abnormal conditions is strictly imperative in order to achieve its lifetime specifications and also fulfil the grid codes. In this paper presents a new control scheme for DFIG wind turbine having parallel interleaved converters (PIC) configuration and a series dynamic braking resistor (SDBR) connected at its stator side. Interleaving the wind turbine converters in parallel configuration could help to increase the current capability, while the SDBR helps in post fault recovery of the wind turbine and also used for used to improve the FRT of large wind farms composed of induction generators. The shorter duration of operation of the SDBR gives a better response of the DFIG system during a grid fault. The coordinated control analysis of the scheme was implemented in power system computer aided design and electromagnetic transient including DC simulation environment for a severe three-phase to ground fault. A better performance of the wind turbine variables were achieved using the proposed control scheme of the PIC and SDBR because the space vector modulation of the PIC results in maximum value of the change in common mode voltage, leading to improved switched output voltage of the voltage source converter leg. Simulation results were obtained compared with the conventional DC chopper and crowbar rotor circuit protection scheme for the wind turbine and also demonstrate that in uncritical post-fault situations the control schemes are able to restore the wind turbines normal operation without disconnections.***

***Index terms-Doubly-fed induction generator (DFIG), series dynamic braking resistor (SDBR), parallel interleaved converters (PIC)***

## I. INTRODUCTION

Wind energy technology has experienced important gains over the last few decades [1] due to the technological improvement of wind turbines from fixed speed to variable speed. There are several types of the wind turbine generators(WTGs), one of which is the Doubly Fed Induction Generator (DFIG). In the last decades, the DFIG has been widely applied in the variable speed constant frequency wind power technology. This is due to its simple control strategy, low losses, and it being capable of regulating the active and reactive power separately. The Doubly Fed Induction Generator (DFIG) has very attractive characteristics as a wind generator in the fast growing market. The fundamental feature of the DFIG is that the power processed by the power converter is only a fraction of the total power rating, that is, typically (20-30%), and therefore its size, cost and losses are much smaller compared to a full size power converter. However, the DFIG suffers from its sensitivity to grid faults, as a result of its direct connection to the grid.

Based on the available wind speed and specific operation requirements, DFIG wind turbine can operate at a wide range of speed. Consequently, it gives room for a better capture of wind energy [2–4]. Besides, it has frequency converters that can operate at high sampling and switching frequencies [5] in its pulse width modulation (PWM), making it superior for independent control of active and reactive power during grid disturbances [6]. Moreover, the dynamic slip control and pitch control are the other important characteristics which help to enhance the system stability of this wind turbine technology. Many techniques have been presented to improve the stability. However, during a grid fault, the DFIG is vulnerable to grid disturbances because the stator windings are connected directly to the grid while the rotor windings are buffered from the grid via a partially-rated frequency converter [2-5]. In [1, 6], a crowbar was used to improve the FRT of DFIG,A static series compensator (SSC) or a dynamic voltage restorer (DVR) [7-9] and STATCOM [10] were used to improve the FRT of the DFIG. A series dynamic braking resistor (SDBR) was used to improve the FRT of large wind farms composed of induction generators in [11], while in [12] the SDBR was connected to the rotor side converter of the DFIG to improve its FRT. The use of superconducting fault current limiter (SFCL) [12], passive resistance network [13], and series anti-parallel thyristor [14] connected to the stator side of a grid connected DFIG, have been reported in the literature.

Since the DFIG wind turbine power converters are vulnerable and fragile during transient conditions, it is imperative to protect and keep the wind turbine in operation to avoid damages. A salient requirement for the DFIG is to inject its three phase rotor circuit with a controllable frequency and magnitude voltage. The AC three phase voltage can be controlled using various switching techniques ranging from six step switching [15], PWM [16], and space PWM [17]. The conventional DFIG system uses two level back to back power converters, which is hardly used for high power applications. Consequently, a multilevel converter using PWM are highly preferred for wind power generation application [18, 19]. The main reason behind this is that the multilevel power converter structure for wind turbines increases the power rating as well as reduces the stress on the insulated-gate bipolar transistors (IGBTs) switches and therefore enhances the voltage waveforms, in addition to reducing the harmonic content. it was established that the harmonic quality of the resultant voltage waveforms in high power applications could be improved by interleaving the carrier signals of the parallel connected VSCs. In [20, 21], the reliability analysis and robustness of MW level IGBT module under short circuit events were carried out, respectively. Power quality improvement for DFIG system using different types of rotor converters was presented in [22], where it was reported that higher harmonic contents occur with the six-step 2 level IGBT inverter due to low switching frequency, thus the performance of this type of inverter system is reduced. This work tends to improve the performance of the conventional two level IGBT back to back power converter of the DFIG

variable speed wind turbine during grid fault by interleaving the converters in parallel configuration in conjunction with a SDBR. The SDBR control strategy in the DFIG wind turbine possess the advantage of providing high voltage that is shared by the resistance due to the series topology of connection. As a result, the loss of power converter control does not occur due to overvoltage that is induced during transient. Moreover, the RSC control synchronism is enhanced during rotor overvoltage, because the SDBR limits high rotor current more significantly to a large extent. Therefore, the charging current of the DC-link capacitor is reduced; consequently this will avoid the DC-link overvoltage which could be harmful to the DFIG variable speed wind turbine power converter system due to loss of control. This work is organised as follows. Section 2 presents a brief description of the conventional DFIG model system having crowbar, DC chopper and SDBR system. The analysis of the proposed parallel interleaved power converters and the SDBR scheme were given in Section 3. In Section 4, a brief was given about the grid requirement for wind farms, while Section 5 shows the simulations in power system computer aided design and electromagnetic transient including DC (PSCAD/EMTDC) [23] environment considering the proposed scheme and conventional schemes in the literature. Section 6 draws the conclusion.

## II WIND TURBINE MODEL AND CONVENTION PROTECTION SCHEMES

### *A. Wind turbine model*

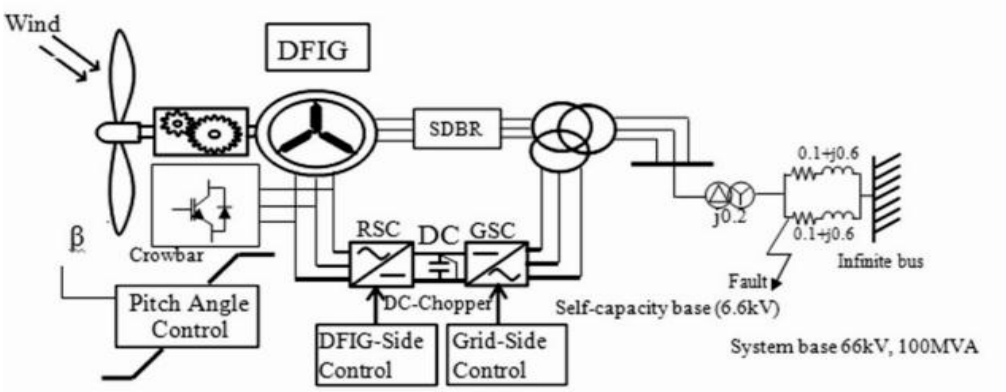


Fig.1. Model system with conventional protection schemes

The dynamics interaction involving forces from the wind and the response of wind turbine determines the amount of kinetic energy that can be extracted. The aerodynamic torque and the mechanical power of a wind turbine are given by [1- 3].

$$T_M = \frac{\pi\rho R^3}{2} V_w{}^2 C_t(\lambda) \quad \text{[N.m]} \qquad (1)$$

$$P_M = \frac{\pi\rho R^2}{2} V_w{}^3 C_p(\lambda) \quad \text{[N..m]} \qquad (2)$$

Where $\rho$ is the air density, R is the radius of the turbine, $V_w$ is the wind speed ,$C_p(\lambda,\beta)$ is the power coefficient given by

$$C_p(\lambda,\beta) = 0.5(\Gamma - 0.02\beta^2 - 5.6)e^{-0.17\Gamma} \qquad (3)$$

The relationship between $C_t$ and $C_p$is

$$C_t(\lambda) = \frac{C_p(\lambda)}{\lambda} \qquad (4)$$

$$\lambda = \frac{w_r R}{V_w} \qquad (5)$$

$$\Gamma = \frac{R(3600)}{\lambda\,(1609)} \qquad (6)$$

Where λ is the tip speed ratio. The wind turbine characteristics[6] for DFIGs are shown in Figs. 2. In Fig. 2, the power capture characteristic of the turbine and the rotor speed are shown. The dotted lines show the locus of the maximum power point of the turbine which is used to determine the reference of active power output ref P .Equations (7) and (8) are used to calculate the reference of the active power output ref P as shown in section A of Fig. 3. The optimum rotor speed ω is given in eqn. (9). The operation range of the rotor of DFIG is chosen from 0.7pu to 1.3pu as shown in the wind turbine characteristics in Fig. 2.

$$P_{ref1} = 0.1571V_w - 1.035 \ \text{[pu]} \qquad (7)$$

$$P_{ref2} = 0.2147V_w - 1.668 \ \text{[pu]} \qquad (8)$$

$$\omega_{reft} = 0.07751V_w \ \text{[pu]} \qquad (9)$$

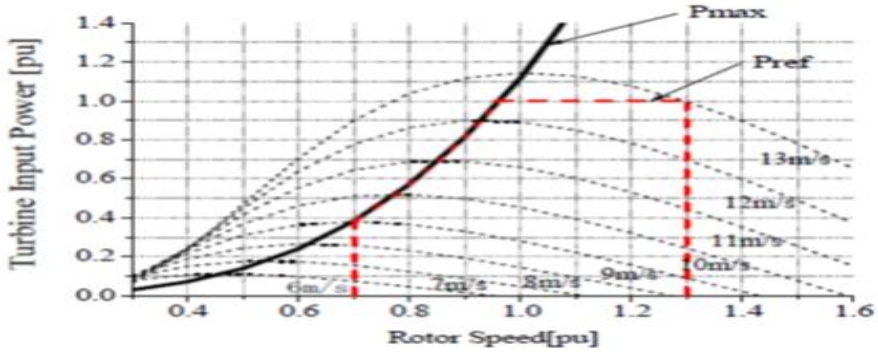


Fig.2 Turbine characteristic with maximum power point tracking for DFIG.

In (7)–(9) Pref1 is the reference active power of the wind turbine during high wind speed,$P_{ref2}$ is the reference active power of thewind turbine during low wind speed and $\omega_{wt\ opt}$ is the optimum wind turbine speed.

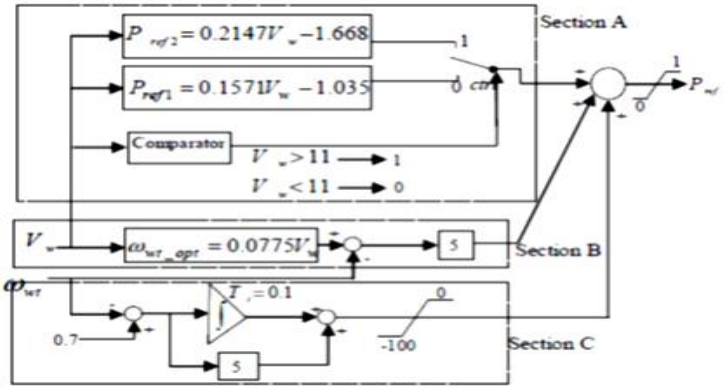


Fig. 3 Control block to determine active power reference $P_{ref}$.

***B. Crowbar circuit***

In order to protect the RSC from over-current damage, the generator rotor circuit is shorted and the RSC is blocked through a crowbar system. There are two types of crowbar systems, passive and active. Active crowbar is more popular because of the fully controllable characteristics [2]. This type of crowbar consists of semiconductor switches such as GTOs or IGBTs. If either the rotor current or DC link voltage levels exceed their limits due to faults, the IGBTs of the RSC are blocked and the active crowbar is turned on. After the fault clearance, the RSC is restarted and the reactive power is ramped up in order to support the grid.

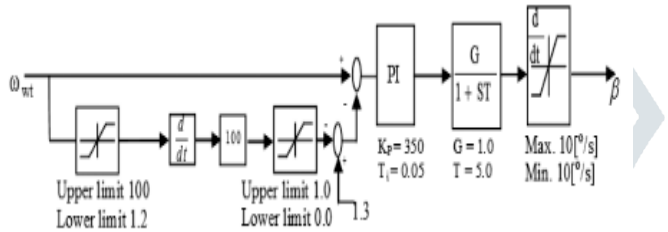


Fig. 4 Pitch controller for DFIG wind turbine

***C. SDBR modelling***

The SDBR contribute directly to the balance of active power during fault. SDBR modelling is accomplished by the insertion of a resistor in the stator circuit. Thus it increases the voltage at the terminal of DFIG and mitigates the destabilizing depression of electrical torque and power during fault [7]. Figure 5 shows schematic diagram of SDBR which is located in the stator side of the generator.

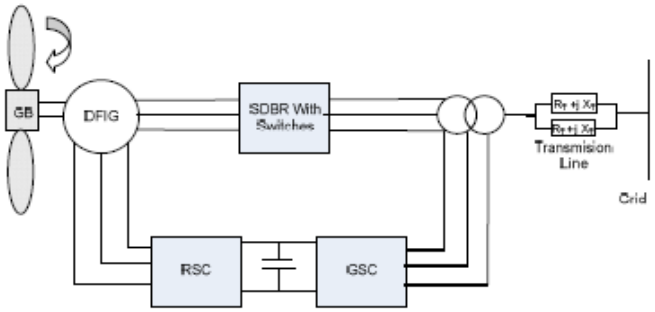


Fig. 5. Model system with SDBR

Fig. 5. Model system with SDBR It can be seen from Fig. 6 that stator voltage Vs is increased due to the insertion of SDBR during fault. Since square of the stator voltage is proportional to mechanical power, SDBR will increase mechanical power and thus improve performance during voltage dip. Thus SDBR can be a very effective mean to enhance the dynamic performance of a DFIG based wind turbine generator.

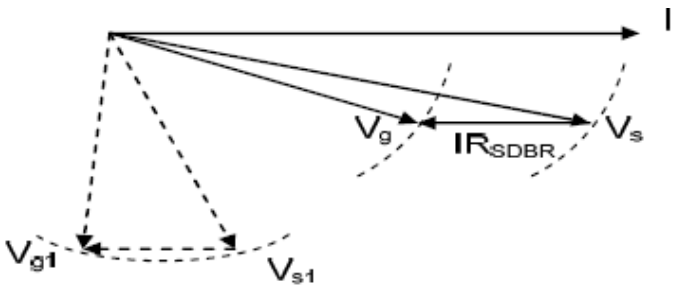


Fig. 6.Phasor diagram with the effect on stator voltage.

## III PROPOSED MODEL SCHEME OF THE STUDY

***A. Dynamics of the parallel interleaved converters (PIC)***

Fig. 7 shows the general structure of the proposed PIC configuration and the SDBR for the DFIG system. The switching table is shown in Fig. 8, where the number represents the switching sequence involved in the near state PWM. The formulation of a reference space vector Vref by the geometrical summation of the three nearest voltage vector in the region 1 is shown in Fig. 9.

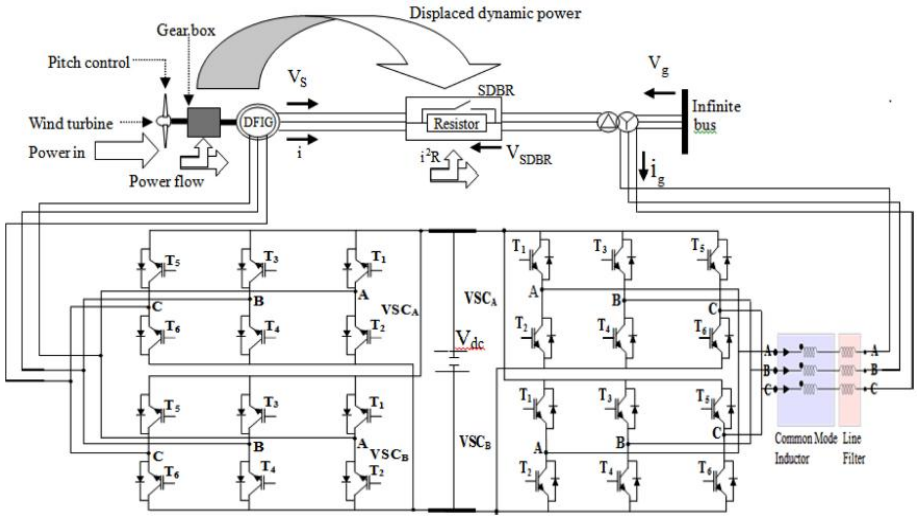


Fig. 7 Proposed schemes for the wind turbine.

The passive grid side filters and their connections to the PIC are shown in Fig. 7. Harmonics can be mitigated by the common mode (CM) inductor and the grid filters of value 9.6mH. The IGBT switches are enumerated for both converter systems.

In the conventional space vector modulation (SVM), the VSC cycles via a four switch states in each switching cycle. For the parallel interleave VSCs, with an interleaving angle of 180°, the use of the SVM results in maximum value of the change in CM voltage to ± Vdc, whereas for the clamped discontinuous PWM schemes, this value is ± (2Vdc/3). The flux in the common leg can be reduced by reducing the time integral of the change in the CM voltage. This is achieved by avoiding the use of zero voltage vectors. This work employs the near state PWM scheme that has three nearest active voltage vectors to synthesise the reference voltage vector Vref. The switching table sequence in Fig. 8 is based on the sequence of numbers in which the corresponding voltage vectors are applied considering the space vector diagram in Fig. 9 which is divided into six regions. The switching sequence 612 is used in both sub-sector 1 where $0° \leq \phi \leq 30°$ and sub-sector 12 where $330° \leq \phi \leq 360°$. Theoretically, these two sub-sectors together make up region 1 and the geometrical formation of the reference voltage Vref in this region is shown in Fig. 7. The active voltage vectors V1, V2 and V6 in the switching table are given as [18]:

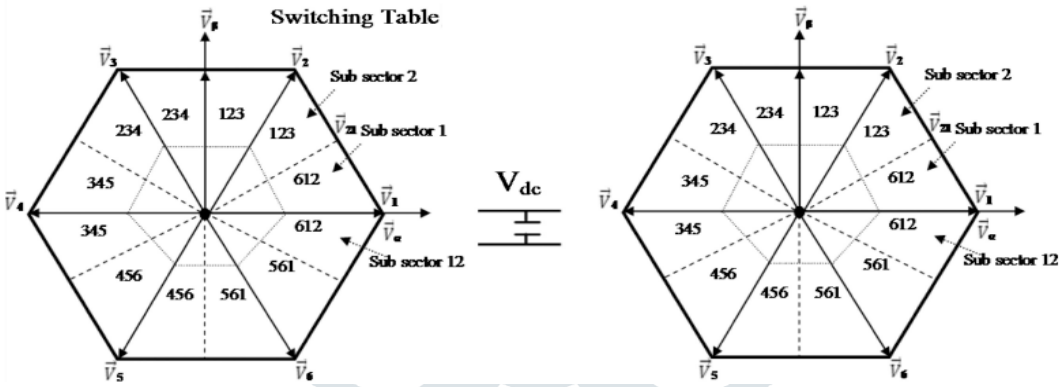


Fig. 8 Switching table of the PIC

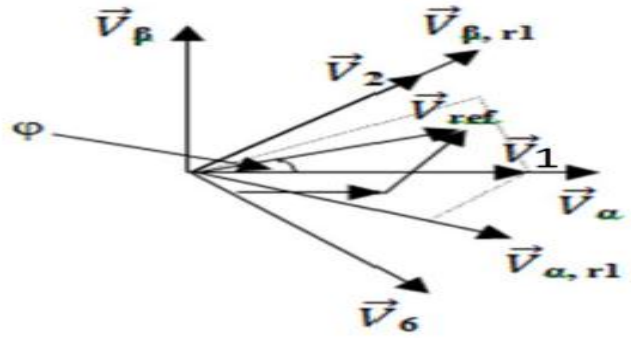


Fig. 9 Formation of the reference space vector $V_{ref}$

$$T_1 = \left(\sqrt{3}\frac{V_{\alpha.r}}{V_{dc}} + \frac{V_{\beta.r}}{V_{dc}} - 1\right)T_s \quad (10)$$

$$T_2 = \left(1 - \frac{2}{\sqrt{3}}\frac{V_{\alpha.r}}{V_{dc}}\right)T_S \quad (11)$$

$$T_6 = \left(1 - \frac{1}{\sqrt{3}}\frac{V_{\alpha.r}}{V_{dc}} - \frac{V_{\beta.r}}{V_{dc}}\right)T_s \quad (12)$$

where, $T_1$, $T_2$ and $T_3$,, are the respective dwell times of the activevoltage vectors, $T_S$ is the switching time, $V_\alpha$, $V_\beta$ are the α, β components represented in Fig. 6 and Vα,r and Vβ,r are the α and β components at the start of the region and these are given for region1 as:

$$V_{\alpha.r1} = \frac{\sqrt{3}}{2}V_\alpha - \frac{1}{2}V_\beta \quad (13)$$

$$V_{\beta.r1} = \frac{1}{2}V_\alpha - \frac{\sqrt{3}}{2}V_\beta \quad (14)$$

$$T_1 = \frac{2}{\sqrt{3}}\frac{|V_{ref}|}{V_{dc}} T_s \sin(60^0 - \varphi) \quad (15)$$

$$T_2 = \frac{2}{\sqrt{3}}\frac{|V_{ref}|}{V_{dc}} T_s \sin(\varphi) \quad (16)$$

$$T_3 = T_6 = {}^{(T_S - T_1 - T_2)}/_2 \quad (17)$$

The dwell time of the adjacent active vectors ($T_1$, $T_2$) for the active zero state PWM is the same as that of the conventional SVM as shown in Eqs (15)–(17). Though in this case, instead of using the zero vectors, two near opposing active voltage vectors ($V_3$, $V_6$) are used consequently, the linear operation over the entire modulation range($0 \leq M \leq 2/3$) is obtained. In the two level converter system only eight voltage vectors that includes two nulls is generated. The complex switching circuitry of the two level interleaved VSC system allows much possibility for appropriate voltage vector selection to satisfy the commutation condition.

The switching sequence and the CM voltages for the proposed DFIG system are shown in Fig. 10 for the parallel interleaved VSCs(A and B) for the rotor and grid side converters (GSCs),respectively. The first half of the converter is tagged A and the second half tagged B, then CM voltage of each VSC are VCM, A and VCM, B, respectively and their difference ΔVCM are shown in Fig. 8. Because only active vectors are used, the peak CM voltage of the individual VSCs is limited to ± ($V_{dc}$/6). The application of voltage vectors $V_1$ and $V_2$ results in equal and opposite polarity CM voltages for the converter system and again because of opposite polarity of the individual CM voltages, the joint application of $V_1$ in $VSC_A$ and $V_2$ in $VSC_B$ and the other way round in sub sector 1 forces the difference in CM voltages ΔVCM to take the value of ± ($V_{dc}$/3). Therefore, for a given dc link voltage, the peak value of the flux linkage in a switching cycle $\lambda_{CM,p}$ depends on the overlap time of the voltage vectors as indicated in Fig. 8. Again, when the $V_{ref}$ is in sub sector 12 as shown in the switching table, the overlap time of the voltage vectors $V_1$ and $V_6$ determines the value of the $\lambda_{CM,p}$, and its value changes with every current state of the reference voltage vector $V_{ref}$ because the reference voltage varies with the space vector angle φ, consequently possessing different values in each switching cycle of the converter system. Therefore, the space vector PWM can be validated from the switching sequence given in Fig. 10 for the 12 switches considering the 12 sub sectors.

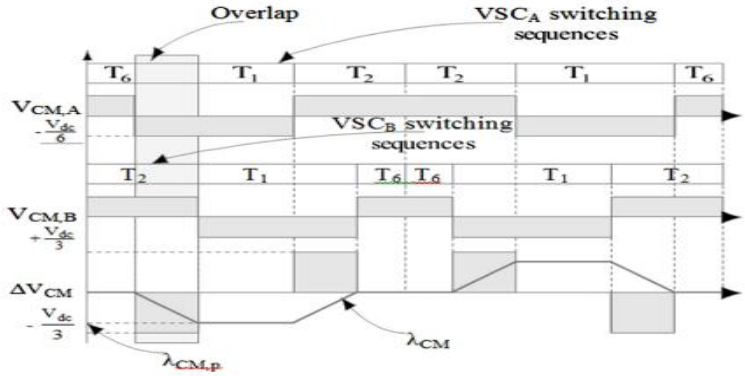


Fig. 10 Switching sequence and CM voltages for VSCs A and B.

## IV GRID CODES

All around the world, the grid codes vary in scope and specific details from one jurisdiction to another. In order to regulate wind farms, all areas have developed specifications according to their relevant technical situations. The literatures [5, 6] have given Wind Power grid specifications in Europe and the Americas. The State Grid Corporation of China have established Wind Power System technical requirements(revised) in February, 2009. The main requirements are summarized below:

(i) Active power. It provides a clear requirement that wind farms must have the ability to regulate the active power, and to control their active power output in accordance with the dispatching department directives.

(ii) Reactive power. The wind farms are required, in any way, to guarantee a certain amount of reactive power regulation capacity. The power factor range is typically between 0.9(lag) to 0.98(lead).

(iii) Voltage range. When the voltage of the point of common connecting deviation between -10%- +10%, the wind turbines should be able to work properly. The wind farms should be able to control the point's voltage between -3%-+7%, within its capacity.

(iv) Frequency operating range. The wind turbines are expected to operate within typical grid frequency variations which the system frequency varies from 49.5 to50.5HZ. (v) Low Voltage Ride Through (LVRT). In the event of a voltage drop, the turbines are required to remain connected for a specific amount of time before being allowed to disconnect. This requirement is to ensure that there is no loss of generation for normally cleared faults. Disconnecting a wind generator too quickly could have a negative impact on the grid, particularly with large wind farms. Fault current contributions from WTGs will have a significant impact on the protection and control of the wind farm as well as the interconnected system. A series dynamic braking resistor (SDBR) was used to improve the FRT of large wind farms composed of induction generators in [15], while in [16] the SDBR was connected to the rotor side converter of the DFIG to improve its FRT.

A small size SBDR can be inserted in series with the stator circuit of the DFIG through the control of power electronic switches to balance the active power, which eventually improves the wind generator stability during a grid fault and isless expensive than the SFCL, passive resistance network and series anti-parallel thyristor.

## V SIMULATION RESULTS

Simulations were run for three scenarios. The first scenario considers the conventional protection scheme for the wind turbine and the proposed PIC scheme. In the second scenario, the coordinated control of the use of the SDBR and PIC in enhancing the DFIG wind turbine. And in the third scenario SFCL is replacing with SDBR was analyzed.

***A. Scenario 1: conventional protection schemes and the proposed scheme for DFIG***

The model system in Fig. 1 was subjected a severe three-phase to ground fault and responses of the DC-link voltage of the wind turbine was observed using the conventional DC-chopper and crowbar schemes. These responses where further compared with that obtained using the proposed parallel interleaved converter scheme as shown in Fig. 11*a*. On basis of the response in Fig. 11*a*, the DC chopper gave a better performance than the expensive crowbar system as reported in the literature because of faster settling time with less oscillations. Hence, the DC chopper would be used for further analysis in this work. When the converters were interleaved based on the switching table in Fig. 6 and the formation of the reference space vector, more current would be in circulation because of the active voltage vectors and their dwell times as described by the equations in Section 3 for the PIC system. A further investigation of interleaving only the RSC or only the GSC was compared with when both sides of the converters were interleaved as shown Fig. 11*b*. Interleaving both converters of the wind turbine creates room for more switching commutation of the IGBTs with increased circulating current and more reactive power provision as shown in Fig. 11*b*. Thus the power converters are more protected during transient conditions.

***B. Scenario 2: Enhancing The DFIG Wind Turbine Using the Proposed Scheme And SDBR***

scenario whereby an SDBR connected to the stator of the DFIG variable speed wind turbine as shown in the model system was further investigated in conjunction with the PIC. Some of the responses are shown in Figs. 11*c* and *d*. The coordinated control of the PIC and SDBR topology improves the performance of DFIG wind turbine because the induced overvoltage caused during transient periods is limited by controlling the rotor overvoltage and same time limits the high rotor current of the wind turbine as described by Eq. (13)–(17). Consequently, the rotor current limitation reduces the charging current to the DC-link capacitor, hence avoiding DC-link overvoltage/under voltage which could damage the DFIG power converter. The SBDR can also balance the active power of the DFIG based on the displaced dynamic power shown in the model system and thus, improves the DFIG wind generator stability during grid fault. Furthermore, the SDBR increases the wind generator output which therefore reduces its speed increase (Fig. 11*c*) during transient periods considering the pharos diagram in Fig. 9. The combination of all these effects improves the terminal voltage (11d) and entire performance of the DFIG system using the proposed scheme. The terminal voltage of the DFIG system in Fig. 11*d* follows the grid requirement (Fig. 10) during transient as it was able to recover within the stipulated time to avoid the shutdown of the wind farm. However, the scenario where the SDBR was implemented gave a fast recovery of the wind turbine terminal voltage. A better performance of the wind turbine terminal voltage was achieved with the coordinated control of the SDBR and PIC proposed strategy.

***C. Scenario 3: Enhancing The DFIG Wind Turbine Using the Proposed Scheme And SDBR and Extension SFCL***

Scenario whereby an SFCL connected to the stator of the DFIG variable speed wind turbine was further investigated in conjunction with the SDBR with PIC. Some of the responses are shown in Figs. 11*a to d*. The coordinated control of the PIC and SFCL topology improves the performance of DFIG wind turbine because the induced overvoltage caused during transient periods is limited by controlling the rotor overvoltage and same time limits the high rotor current of the wind turbine as described by Eq. (14)–(18). Consequently, the rotor current limitation reduces the charging current to the DC-link capacitor, hence avoiding DC link overvoltage/under voltage which could damage the DFIG power converter. When SFCL has an impedance of 10 and 20 Ω, respectively. The results showed fault current limiting characteristics and improvement in voltage unbalance. In addition, we discovered following features: 1) the larger resistance of a resistor-type SFCL, the more voltage unbalance was improved. 2) In SFCL operating process, there are differences of recovery time between superconducting elements owing to unbalance fault current shown in Fig. 11(a)-(d). If a fault occurs, the proposed method clears voltage unbalance and protects can also balance the active power of the DFIG and thus, improves the DFIG wind generator stability during grid fault. A better performance of the wind turbine terminal voltage was achieved with the coordinated control of the SFCL and PIC extension strategy.

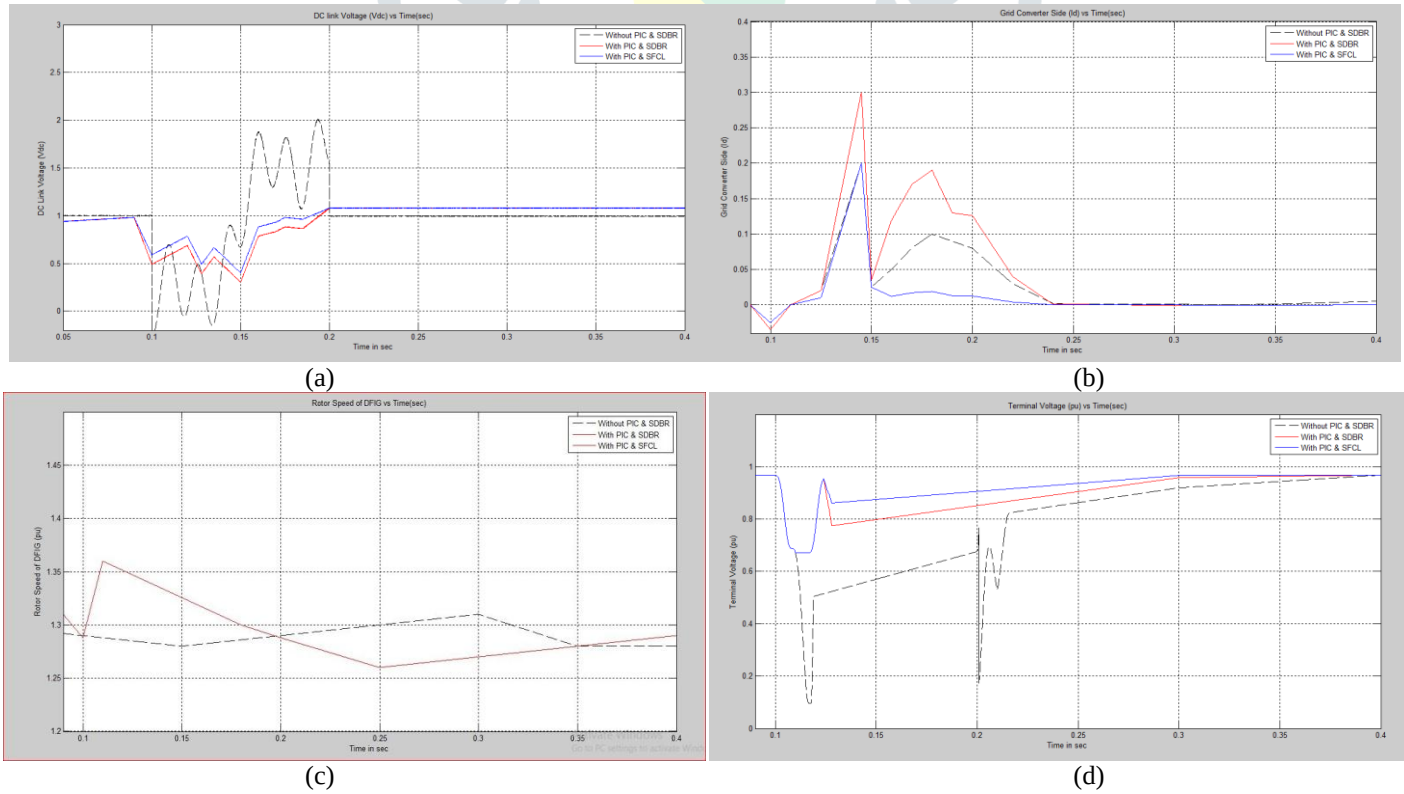


(a) (b)

(c) (d)

Fig. 11 Proposed parallel interleaved converter scheme
(a) DC-link voltage of DFIG, (b) GSC of DFIG, (c) Rotor speed of DFIG, (d) Terminal voltage of DFIG

## VI CONCLUSION

The performance of Doubly Fed Induction Generator (DFIG) variable speed wind turbine with parallel interleaved VSCs and a dynamic resistor was investigated during a grid fault. Interleaving the carrier signals in parallel configuration of the VSC system in a variable speed wind turbine can improve its performance during transient conditions. This is because, it allows for much more possibilities of appropriate voltage vector selection to enhance switching and commutation condition. To further enhance the performance of the DFIG wind turbine, a coordinated control of the parallel interleaved converter and a SDBR of low value were suggested. The performance of the wind turbine was analyzed considering a severe three-phase to ground fault to test the rigidity of the wind turbine system. The simulation results presented show improved performance of the variable speed wind turbine system using the proposed scheme. And extension was developed by using SFCL with PIC, following features: 1) the larger resistance of a resistor-type SFCL, the more voltage unbalance was improved. 2) In SFCL operating process If a fault occurs, the proposed method clears voltage unbalance and protects can also balance the active power of the DFIG and thus, improves the DFIG wind generator stability during grid fault. A better performance of the wind turbine terminal voltage was achieved with the coordinated control of the SFCL and PIC extension strategy.

## REFERENCES


**[1]** *Kenneth E. Okedu*, "Enhancing DFIG wind turbine during three phase fault using parallel interleaved converters and dynamic resistor," *IET Renew. Power Gener.*, 2016, available online IEEE Explorer.

**[2]** K. E. Okedu, S. M. Muyeen, R. Takahashi, and J. Tamura, "Stabilization of wind farms by DFIG-based variable speed wind generators," International Conference on Electrical Machines and Systems (ICEMS), Seoul, South Korea, 2010, available online IEEE Explorer.

**[3]** S. Santos, and H. T. Le, "Fundamental Time-Domain Wind Turbine Models for Wind Power Studies," Renewable Energy, Vol. 32, pp. 2436- 2452, 2007.

**[4]** Johan Morren , Sjoerd W. H. de Haan " Ride through of Wind Turbines with Doubly-Fed Induction Generator During a Voltage Dip" IEEE Transaction on energy conversion, VOL. 20, NO. 2, JUNE 2005 435-441.

**[5]** A. Causebrook, D. J. Atkinson, and A. G. Jack, "Fault ride through of large wind farms using series dynamic braking resistors," IEEE Trans. Power Systems, vol. 22, no. 3, pp. 966-975, March, 2007. [16] J. Yang, E. Fletcher, and J. O'Reilly,"A series dynamic

**[6]** Santos, S., Le, H.T.: 'Fundamental time-domain wind turbine models for wind power studies', Renew. Energy, 2007, 32, pp. 2436–2452

**[7]** Chowdhury, B.H., Chellapilia, S.: 'Doubly-fed induction generator control for variable speed wind power generation', Electr. Power Syst. Res., 2006, 76, pp. 786–800

**[8]** Karim-Davijani, H., Sheikjoleslami, A., Livani, H., et al.: 'Fuzzy logic control of doubly fed induction generator wind turbine', World Appl. Sci. J., 2009, 6, (4), pp. 499–508

**[9]** Sun, T., Chen, Z., Blaabjerg, F.: 'Transient stability of DFIG wind turbines at an external short circuit fault', Wind Energy J., 2005, 8, pp. 345–360.

**[10]** Murphy, J., Turnbull, F.: 'Power electronics control of AC motors' (Pergamon, New York, 1988)

**[11]** Muller, S., Deicke, M., Doncker, R.W.D.: 'Doubly fed induction generator systems for wind turbine', IEEE Ind. Appl. Mag., 2002, 8, (3), pp. 26–33

**[12]** Mohan, N.: 'First course on power electronics' (MNPERE/Prentice-Hall, Englewood Cliffs, 2005)

**[13]** Akahashi, I. Akagi, H.: 'A new neutral point clamped PWM inverter', IEEE Trans. Ind. Appl., 1981, 17, pp. 518–523

**[14]** Stemmler, H., Geggenbach, P.: 'Configurations of high power voltage source inverter drives'. Proc. of the 5th European Conf. on Power Electronics and Applications, Brighton, UK, 1993, 5, pp. 7–12

**[15]** Muller, S., Deicke, M., Doncker, R.W.D.: 'Doubly fed induction generator systems for wind turbine', IEEE Ind. Appl. Mag., 2002, 8, (3), pp. 26–33

**[16]** Zhang, D., Wang, F., Burgos, R., et al.: 'Impact of interleaving on AC passive components of paralleled three phase voltage source converters', IEEE Trans. Power Electron., 2010, 46, (3), pp. 1042–1054

**[17]** Ma, K., Zhou, D., Blaabjerg, F.: 'Evaluation and design tools for the reliability of wind power converter system', J. Power Electron., 2015, 15, (5), pp. 1149–1157

**[18]** Reigosa, P.D., Wu, R., Iannuzzo, F., et al.: 'Robustness of MW level IGBT modules against gate oscillations under short circuit events', Microelectron. Reliab., 2015, 55, pp. 1950–1955

**[19]** PSCAD/EMTDC Manual: Manitoba HVDC Research Center, 1994

**[20]** E.ON NETZ GmbH: 'Grid connection regulation for high and extra high voltage'. 2006

**[21]** Stemmler, H., Geggenbach, P.: 'Configurations of high power voltage source inverter drives'. Proc. of the 5th European Conf. on Power Electronics and Applications, Brighton, UK, 1993, 5, pp. 7–12

**[22]** Gohil, G., Bede, L., Teodorescu, R., *et al.*: 'An integrated inductor for parallel interleaved VSCs and PWM schemes for flux minimization', *IEEE Trans. Ind. Electron.*, 2015, **62**, (12), pp. 7534–7546

**[23]** Ueda, F., Matsui, K., Asao, M., *et al.*: 'Parallel connections of pulse width modulated inverters using current sharing reactors', *IEEE Trans. Power Electron.*, 1995, **10**, (6), pp. 673–679